

Pyridyl-Substituted Thioaminy Stable Free Radicals: Isolation, ESR Spectra, and Magnetic Characterization¹

Yoza Miura,* Shinya Kurokawa, and Masaaki Nakatsuji

Department of Applied Chemistry, Faculty of Engineering, Osaka City University,
Sumiyoshi-ku, Osaka 558-8585, Japan

Kenjiro Ando and Yoshio Teki*

Department of Material Science, Graduate School of Science, Osaka City University,
Sumiyoshi-ku, Osaka 558-8585, Japan

Received June 16, 1998

N-[(4-Nitrophenyl)thio]- (**1a**) and *N*-[(2,4-dichlorophenyl)thio]-2,6-diphenyl-4-(3-pyridyl)phenylaminy (**1b**), *N*-[(4-nitrophenyl)thio]- (**2a**) and *N*-[(2,4-dichlorophenyl)thio]-4-phenyl-2,6-di(3-pyridyl)phenylaminy (**2b**), and *N*-[(2,4-dichlorophenyl)thio]-2,6-diphenyl(4-pyridyl)aminy (**3**) were generated by PbO₂ oxidation of the corresponding precursors. Although **3** was not sufficiently stable to be isolated, both **1** and **2** persisted in solution without decomposition and could be isolated as radical crystals. X-ray crystallographic analysis of **1b** revealed that the Ar–N–S–Ar' π -framework is approximately planar and the 2- and 6-phenyl groups are significantly twisted from this plane. The magnetic susceptibility measurements for the isolated radical crystals were carried out using a SQUID magnetometer in the temperature range 1.8–300 K. The susceptibilities of **1a** and **2a** were explained in terms of a one-dimensional (1D) antiferromagnetic (AFM) regular Heisenberg model with an exchange interaction of $2J/k_B = -63.4$ and -17.8 K, respectively, and that of **1b** was interpreted in terms of a 1D AFM alternating Heisenberg model with $2J/k_B = -12.8$ K and α (alternation parameter) = 0.91. On the other hand, that of **2b** was explained in terms of a 1D ferromagnetic regular Heisenberg model with $2J/k_B = 22.4$ K.

Introduction

Since the discovery of the first purely organic ferromagnet with $T_c = 0.60$ K in 1991,² magnetism of stable free radical crystals has attracted much attention. Since the discovery of the first organic ferromagnet, a variety of stable free radical crystals have been investigated, and 18 kinds of organic ferromagnets have been found.^{3–14} However, since free radicals are inherently unstable,

examples of isolable free radicals are seriously limited,¹⁵ and the free radicals whose magnetism has been investigated have been almost limited to nitroxide and nitronyl nitroxides. Therefore, the quest of a new class of stable free radicals is strongly desired for the further advances in chemistry and physics of purely organic magnetism. Standing on this background, we have made an effort to search for a new class of isolable stable free radicals,¹⁶ and it has been found that *N*-(arylthio)-2,4,6-triarylphenylaminy and their derivatives are isolable stable free radicals.^{17–20} Magnetic studies of the thioaminy radical crystals have shown that four radicals crystals couple ferromagnetically with $2J/k_B = 3.6–28.0$ K.²¹

(1) ESR Studies of Nitrogen-Centered Free Radicals. 51. For part 50, see: Miura, Y.; Momoki, M. *J. Chem. Soc., Perkin Trans. 2* **1998**, 1185.

(2) (a) Kinoshita, M.; Turek, P.; Tamura, M.; Nozawa, K.; Shiomi, D.; Nakazawa, Y.; Ishikawa, M.; Takahashi, M.; Awaga, K.; Inabe, T.; Maruyama, Y. *Chem. Lett.* **1991**, 1225. (b) Tamura, M.; Nakazawa, Y.; Shiomi, D.; Nozawa, K.; Hosokoshi, Y.; Ishikawa, M.; Takahashi, M.; Kinoshita, M. *Chem. Phys. Lett.* **1991**, 186, 401. (c) Nakazawa, Y.; Tamura, M.; Shirakawa, N.; Shiomi, D.; Takahashi, M.; Kinoshita, M.; Ishikawa, M. *Phys. Rev.* **1992**, B46, 8906.

(3) (a) Chiarelli, R.; Rassat, A.; Rey, P. *J. Chem. Soc., Chem. Commun.* **1992**, 1081. (b) Chiarelli, R.; Novak, M. A.; Rassat, A.; Tholence, J. L. *Nature* **1993**, 363, 147.

(4) Nogami, T.; Tomioka, K.; Ishida, T.; Yoshikawa, H.; Yasui, M.; Iwasaki, F.; Iwamura, H.; Takeda, N.; Ishikawa, M. *Chem. Lett.* **1994**, 29.

(5) Ishida, T.; Tsuboi, H.; Nogami, T.; Yoshikawa, H.; Yasui, M.; Iwasaki, F.; Iwamura, H.; Takeda, N.; Ishikawa, M. *Chem. Lett.* **1994**, 919.

(6) Nogami, T.; Ishida, T.; Tsuboi, H.; Yoshikawa, H.; Yamamoto, H.; Yasui, M.; Iwasaki, F.; Iwamura, H.; Takeda, N.; Ishikawa, M. *Chem. Lett.* **1995**, 635.

(7) Nogami, T.; Ishida, T.; Yasui, M.; Iwasaki, F.; Takeda, N.; Ishikawa, M.; Kawakami, T.; Yamaguchi, K. *Bull. Chem. Soc. Jpn.* **1996**, 69, 1841.

(8) Togashi, K.; Imachi, R.; Tomioka, K.; Tsuboi, H.; Ishida, T.; Nogami, T.; Takeda, N.; Ishikawa, M. *Bull. Chem. Soc. Jpn.* **1996**, 69, 2821.

(9) (a) Sugawara, T.; Matsushita, M. M.; Izuoka, A.; Wada, N.; Takeda, N.; Ishikawa, M. *J. Chem. Soc., Chem. Commun.* **1994**, 1723. (b) Matsushita, M. M.; Izuoka, A.; Sugawara, T.; Kobayashi, T.; Wada, N.; Takeda, N.; Ishikawa, M. *J. Am. Chem. Soc.* **1997**, 119, 4369.

(10) Cirujeda, J.; Mas, M.; Molins, E.; de Panthou, F. L.; Laugier, J.; Park, J. G.; Paulsen, C.; Rey, P.; Rovira, C.; Veciana, J. *J. Chem. Soc., Chem. Commun.* **1995**, 709.

(11) Caneschi, A.; Ferraro, F.; Gatteschi, D.; Lirzin, A.; Novak, M. A.; Rentschler, E.; Sessoli, R. *Adv. Mater.* **1995**, 7, 476.

(12) (a) Mukai, K.; Konishi, K.; Nedachi, K.; Takeda, K.; *J. Magn. Mater.* **1995**, 140–144, 1449. (b) Mukai, K.; Nedachi, K.; Takiguchi, M.; Kobayashi, T.; Amaya, K.; *Chem. Phys. Lett.* **1995**, 238, 61. (c) Mukai, K.; Konishi, K.; Nedachi, K.; Takeda, K. *J. Phys. Chem.* **1996**, 100, 9658.

(13) Takeda, K.; Hamano, T.; Kawae, T.; Hidaka, M.; Takahashi, M.; Kawasaki, S.; Mukai, K. *J. Phys. Soc. Jpn.* **1995**, 64, 2343.

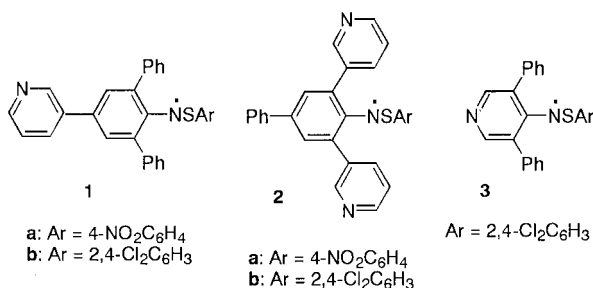
(14) Sugimoto, T.; Tsuji, M.; Suga, T.; Hosoi, N.; Ishikawa, M.; Takeda, N.; Shiro, M. *Mol. Cryst. Liq. Cryst.* **1995**, 272, 183.

(15) (a) Forrester, A. R.; Hay, J. M.; Thomson, R. H. *Organic Chemistry of Stable Free Radicals*; Academic Press: London and New York, 1968. (b) Rozantsev, E. G. *Free Nitroxide Radicals*; Prentice Hall: New York and London, 1970. (c) Volodarsky, L. B.; Reznikov, V. A.; Ovcharenko, V. I. *Synthetic Chemistry of Stable Nitroxides*; CRC Press: Boca Raton, 1994.

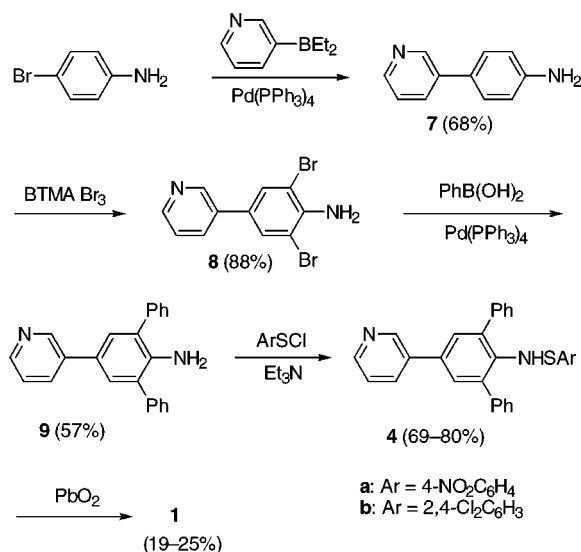
(16) Miura, Y. *Tren. Org. Chem.* **1997**, 6, 197.

(17) (a) Miura, Y.; Tanaka, A. *J. Chem. Soc., Chem. Commun.* **1990**, 441. (b) Miura, Y.; Tanaka, A.; Hirotsu, K. *J. Org. Chem.* **1991**, 56, 6638. (c) Miura, Y.; Kitagishi, Y.; Ueno, S. *Bull. Chem. Soc. Jpn.* **1994**, 67, 3282.

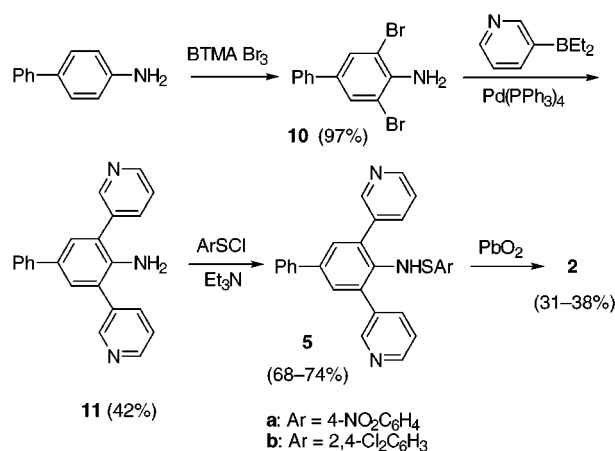
Chart 1



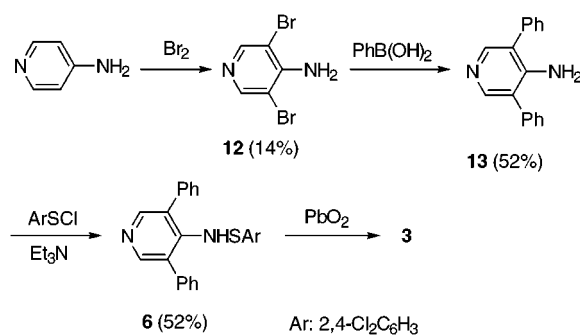
Scheme 1



Scheme 2



Scheme 3



In the present work five kinds of pyridyl-substituted thioaminy radicals, **1a**, **1b**, **2a**, **2b**, and **3** (see Chart 1), were investigated. Of the five radicals investigated, the former four radicals could be isolated as radical crystals, and one of them (**1b**) was investigated by X-ray crystallography. The magnetic studies for the isolated radical crystals have shown that, although the magnetic behaviors of **1a**, **1b**, and **2a** are antiferromagnetic (AFM), that of **2b** is ferromagnetic (FM). Herein we report isolation, ESR spectra, X-ray crystallographic analysis, and magnetic characterization for the isolated four radicals.

Results and Discussion

Preparation of Precursors. Precursor **4** was prepared according to Scheme 1. Thus, the Pd-catalyzed cross-coupling reaction of 4-bromoaniline with diethyl-(3-pyridyl)borane gave **7** in 68% yield.^{22,23} Bromination of **7** was carried out by treating **7** with 3 equiv of benzyltrimethylammonium tribromide (BTMA·Br₃),²⁴ giving

8 in 88% yield. The Pd-catalyzed cross-coupling reaction of **8** with 2.6 equiv of phenylboronic acid gave **9** in 57% yield. Reaction of **9** with 4-nitro- or 2,4-dichlorobenzenesulfonyl chloride in the presence of Et₃N gave **4** in 69–80% yields. Preparation of **5** is described in Scheme 2. Treatment of 4-aminobiphenyl with 2.2 equiv of BTMA·Br₃ gave **10** in 97% yield. The Pd-catalyzed cross-coupling reaction of **10** with 2.4 equiv of diethyl-(3-pyridyl)borane gave **11** in 42% yield. Reaction of **11** with 4-nitro- or 2,4-dichlorobenzenesulfonyl chloride in the presence of Et₃N gave **5** in 68–74% yields. In Scheme 3, preparation of **6** is described. Bromination of 4-aminopyridine with Br₂ gave **12** in 14% yield. The low yield of **12** can be ascribed to the low reactivity of the pyridyl group for electrophilic substitution. The Pd-catalyzed cross-coupling reaction of **12** with 2.6 equiv of phenylboronic acid gave **13** in 52% yield. The reaction of **13** with 2,4-dichlorobenzenesulfonyl chloride in the presence of Et₃N gave **6** in 52% yield.

Generation and Isolation of Radicals. Oxidation of **4**, **5**, and **6** was carried out in benzene with PbO₂. When PbO₂ was added to a stirred solution of **4**, **5**, or **6**, an initially light yellow (**4a**, **5a**) or colorless solution (**4b**, **5b**, **6**) immediately turned green (**1b**, **2a**, **2b**), yellowish green (**1a**), or purple (**3**), and intense ESR signals were observed from the solutions. Although **3** was gradually decomposed in solution ($\tau_{1/2} \sim 8$ h at 20 °C), **1a**, **1b**, **2a**, and **2b** persisted without decomposition over a long period, even in the presence of atmospheric oxygen, and showed no tendency to dimerize on cooling to low temperature. From these observations we decided to try their isolation.

(18) (a) Miura, Y.; Yamano, E.; Tanaka, A.; Ogo, Y. *Chem. Lett.* **1992**, 1831. (b) Miura, Y.; Yamano, E.; Tanaka, A.; Yamauchi, J. *J. Org. Chem.* **1994**, *59*, 3294. (c) Miura, Y.; Yamano, E. *J. Org. Chem.* **1995**, *60*, 1070. (d) Miura, Y.; Oka, H.; Yamano, E.; Teki, Y.; Takui, T.; Itoh, K. *Bull. Chem. Soc. Jpn.* **1995**, *68*, 1187.

(19) Miura, Y.; Fuchikami, T.; Momoki, M. *Chem. Lett.* **1994**, 2127. (b) Miura, Y.; Momoki, M.; Fuchikami, T.; Teki, Y.; Mizutani, H. *J. Org. Chem.* **1996**, *61*, 4300.

(20) Miura, Y.; Momoki, M.; Nakatsuji, M.; Teki, Y.; Itoh, K. *J. Org. Chem.* **1998**, *63*, 1555.

(21) Teki, Y.; Itoh, K.; Okada, A.; Yamakage, H.; Kobayashi, T.; Amaya, K.; Kurokawa, S.; Ueno, S.; Miura, Y.; *Chem. Phys. Lett.* **1997**, *270*, 573.

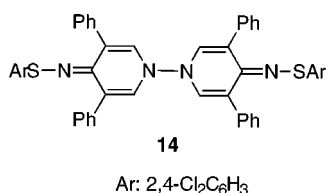
(22) Miura, Y.; Oka, H.; Momoki, M. *Synthesis* **1995**, 1419.

(23) Miyaura, N.; Suzuki, A. *Chem. Rev.* **1995**, *95*, 2457.

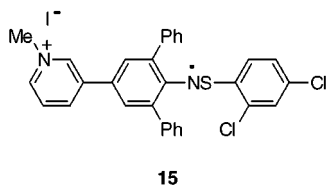
(24) Kajigaeshi, S.; Kakinami, T.; Inoue, K.; Kondo, M.; Nakamura, H.; Fujikawa, M.; Okamoto, T.; *Bull. Chem. Soc. Jpn.* **1988**, *61*, 597.

Isolation of **1a**, **1b**, **2a**, and **2b** was carried out as follows: the precursors were treated with PbO₂ in benzene and, after filtration, the solvent was removed by freeze-drying. The resulting dark green or blue crystalline residue was crystallized from hexane–ethyl acetate (**1a**, **1b**, and **2b**) or EtOH (**2a**) to give radical crystals in 19–38% yields. The IR spectra showed no presence of a NH group, and the elemental analyses agreed with the calculations. The magnetic susceptibility measurements carried out with a SQUID magnetometer showed >93% purity for the isolated radicals (see below).

Radical **3** was shown to be in equilibrium with a dimer. When a solution of **3** in toluene was cooled to –78 °C, the characteristic purple color faded a little, and on warming the solution to room temperature, the original purple color was recovered; this cycle was completely repeated. If the equilibrium constant ($= [\text{radical}]^2/[\text{dimer}]$) for the dimer $\rightleftharpoons 2$ radicals is small, the characteristic purple color will completely disappear. In this case the color faded only a little, suggesting that the equilibrium constant is substantially large. Effort was paid to isolate the dimer, but no pure dimer could be obtained. We assume that the dimer has a structure represented by **14** because the possible coupling position is only the pyridyl nitrogen.



Preparation of a quaternary ammonium salt of **1b**, **15**, was attempted. To an ethyl acetate solution of **1b** was added an excess of MeI, and the resulting solution was allowed to stand for 3 days at 0 °C to give a dark green crystalline powder in 55% yield. Unfortunately, the elemental analysis of the salt did not satisfactorily agree with the calculation,²⁵ and the magnetic susceptibility measurements showed that spin concentration was 50% of the theoretical value. Although the salt showed a weak FM interaction in SQUID measurements, further detailed investigation was not carried out because of its equivocal structure.



ESR and UV–Vis Spectra. A typical ESR spectrum is shown in Figure 1, and ESR parameters for the radicals are summarized in Table 1. Radical **1a** gave an ESR spectrum consisting of a broad 1:1:1 triplet with $a_N = 0.893$ mT ($g = 2.0055$), as shown in Figure 1. Radicals **1b**, **2a**, and **2b** also gave a similar 1:1:1 triplet ESR spectrum, and no further hyperfine splittings were observed for these radicals. This is ascribed to the presence of many unresolved protons with small hyper-

(25) The elemental analysis for the quaternary ammonium salt of **1b**: calcd for C₃₀H₂₂Cl₂IN₂S: C, 56.27; H, 3.46; N, 4.37. Found: C, 53.94; H, 4.15; N, 3.63.

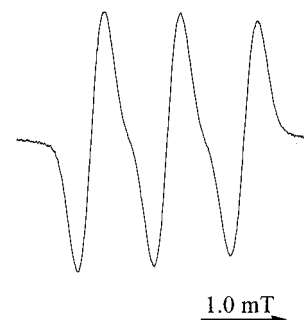


Figure 1. ESR spectrum of **1a** in benzene at 20 °C.

Table 1. ESR Parameters for **1a**, **1b**, **2a**, **2b**, **3**, **18**, and **19** in Benzene at 20 °C^a

radical	a_N	g
1a	0.893	2.0055
1b	0.891	2.0056
2a	0.890	2.0055
2b	0.892	2.0056
3^{b,c}	0.940	2.0065
18	0.889	2.0056
19^{b,d}	0.894	2.0056
20a	0.890	2.0054
20b	0.895	2.0055

^a The hfc constants are given in mT. ^b The hfc constants are determined by computer simulation. ^c The hfc constants for the pyridyl nitrogen and pyridyl meta (2H) and phenylthiyl ortho (1H) protons are 0.172, 0.111, and 0.089 mT, respectively. ^d The hfc constants for the anilino meta (2H) and phenylthiyl ortho (1H) protons are 0.133 and 0.089 mT, respectively.

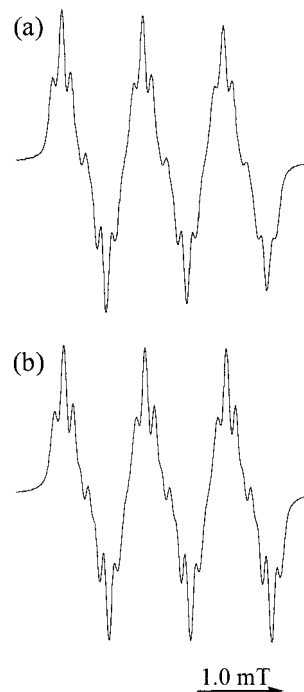


Figure 2. ESR spectrum of **3** in benzene at 20 °C: (a) experimental; (b) computer simulation.

fine splittings. In the case of **3** the 1:1:1 triplet was further split by the interaction with protons and nitrogen, though their splittings were poor (Figure 2). Computer simulation of this spectrum gave $a_N = 0.940$ (1N) and 0.172 mT (1N) and $a_H = 0.111$ (2H) and 0.089 mT (1H). The nitrogen hyperfine coupling (hfc) constant of 0.940 mT is assigned to the NS nitrogen and that of 0.172 mT to the pyridyl nitrogen. On the other hand, the proton

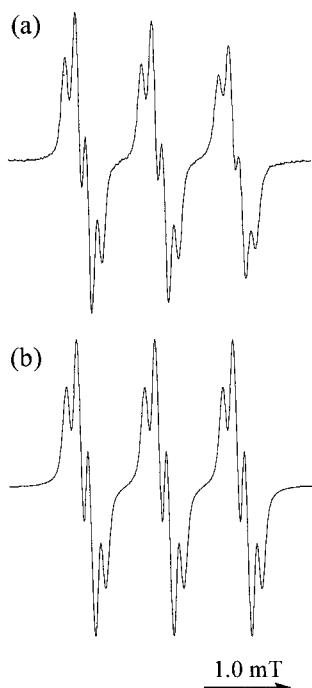
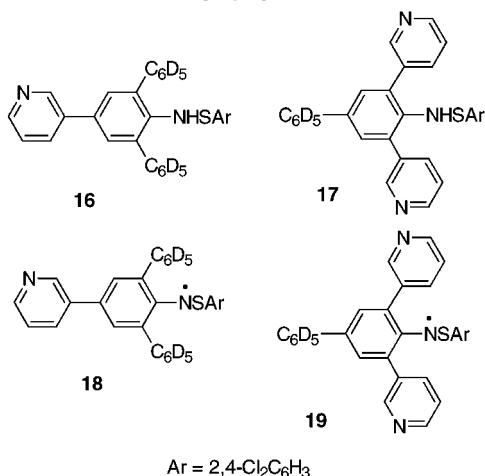


Figure 3. ESR spectrum of **19** in benzene at 20 °C: (a) experimental; (b) computer simulation.

Chart 2



hfc constant of 0.111 mT is assigned to the pyridyl meta protons and that of 0.089 mT to the phenylthiyl ortho proton.

Deuteration of the 2-, 4-, and 6-phenyl groups in **1a**, **2a**, **1b**, and **2b** may render the broad ESR lines sharp because the hfc constants for deuteriums are 0.154 times those of corresponding protons. This may lead to appearance of hyperfine splittings due to the pyridyl nitrogen or protons. Deuteration of the 2-, 4-, and 6-phenyl groups was performed for **1b** and **2b** (Chart 2). The corresponding precursors **16** and **17** were prepared by the same procedure as for **4** and **5**, starting from 2,6-di(phenyl-*d*₅)-4-(3-pyridyl)aniline or 4-(phenyl-*d*₅)-2,6-di(3-pyridyl)aniline. Although the ESR spectrum of **18** was still broad and no hyperfine splittings due to protons were observed, that of **19** was split into 1:3:3:1 quartets of a 1:1:1 triplet, as shown in Figure 3. Computer simulation of the spectrum gave a hfc constant of 0.133 mT for the anilino meta protons (2H) and a hfc constant of 0.089 mT for the phenylthiyl ortho proton (1H). No reduction in the line width observed for the ESR spectrum of **18**

Scheme 4

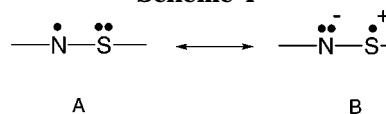
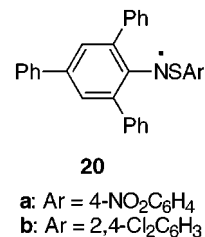


Table 2. UV-Vis Spectroscopic Data of **1a**, **1b**, **2a**, **2b**, and **3** in Benzene

radical	λ_{\max} , nm (ϵ , L mol ⁻¹ cm ⁻¹)
1a	630 (7680), 502 (7560), 430 (16700), 378 (13800), 330 (14800)
1b	636 (8480), 542 (3340 sh), 450 (6440 sh), 394 (21000), 333 (11600)
2a	637 (8410), 502 (5790), 428 (15400), 377 (13800), 336 (12300)
2b	644 (9520), 534 (2210), 448 (4210 sh), 391 (21000), 343 (11500)
3	610, 554

suggests very small or negligibly small delocalization of the unpaired electron onto the 2- and 6-phenyl groups.

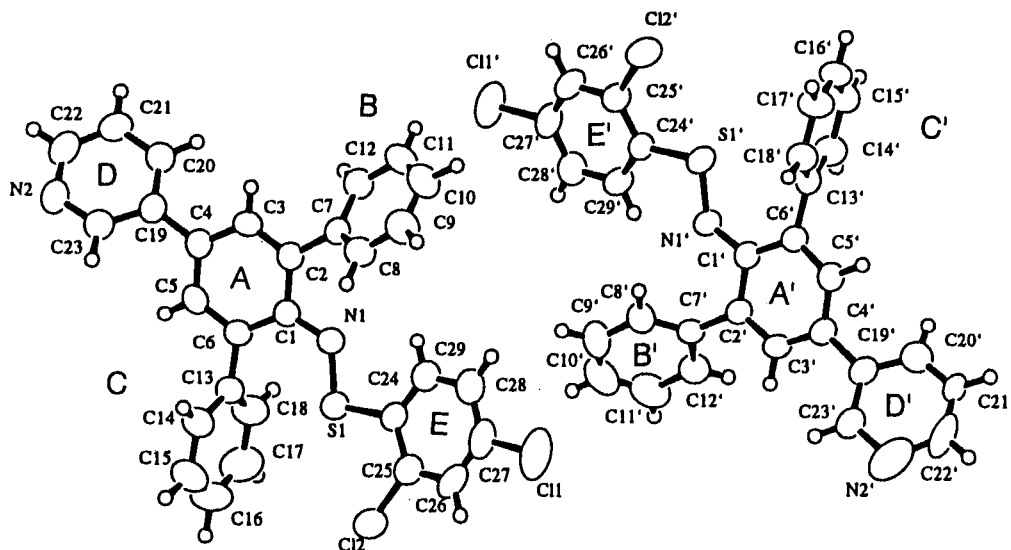
From the above ESR results, the following conclusions are drawn. First, the unpaired electron resides mainly on the Ar-N-S-Ar' π -system, with a greater delocalization of the unpaired electron onto the anilino benzene ring. Second, there is a small delocalization of the unpaired electron onto the 4-phenyl or 4-(3-pyridyl) group. Third, delocalization of the unpaired electron onto the 2- and 6-phenyl or pyridyl groups is very small or negligibly small. This spin density distribution profile is nearly identical to that for *N*-(arythio)-2,4,6-triarylphenylaminyls.¹⁷ For comparison, those for **20a** and **20b** are shown in Table 1.



The a_N and g values for **3** are somewhat different from those for **1a**, **1b**, **2a**, and **2b**. The a_N value for **3** is ~0.05 mT larger than those for **1a**, **1b**, **2a**, and **2b**, and its g value is also ~0.001 higher than those for **1a**, **1b**, **2a**, and **2b**. The absence of the 4-phenyl or 4-(3-pyridyl) substituent must increase a_N . On the other hand, direct attachment of the 4-pyridyl group to the radical center will enhance the canonical form B relative to canonical form A (see Scheme 4) because the 4-pyridyl group is a stronger electron-withdrawing group than phenyl. This leads to a reduction in a_N and an increase in g . Although the magnitude of a_N is changed by the two opposite effects, the increased a_N of **3** shows predominance of the former effect.

Radicals **1**, **2**, and **3** show a characteristic green (**1a**, **2a**, **2b**), yellowish green (**1b**), or purple color (**3**) in solution. The UV-vis spectroscopic data of the radicals are shown in Table 2. Since all radicals show strong absorption peaks attributable to the green or blue color in the visible region, we can readily know the presence of the radicals from the color.

X-ray Crystallographic Analysis. Although **1a**, **1b**, and **2b** crystallized to microcrystals, **1b** provided a sufficiently large single crystal for X-ray crystallography.

Figure 4. ORTEP drawing of **1b**.Table 3. Selected Bond Lengths and Angles and Torsion Angles for **1b**

	syn-form		anti-form
Bond Lengths (Å)			
C1–N1	1.366(4)	C1'–N1'	1.372(4)
N1–S1	1.630(3)	N1'–S1'	1.624(3)
S1–C24	1.766(3)	S1'–C24'	1.770(3)
Bond Angles (deg)			
C2–C1–N1	114.7(3)	C2'–C1'–N1'	113.9(3)
C6–C1–N1	127.2(3)	C6'–C1'–N1'	127.8(3)
C1–N1–S1	123.1(2)	C1'–N1'–S1'	123.4(2)
N1–S1–C24	99.3(2)	N1'–S1'–C24'	98.9(2)
S1–C24–C25	118.3(3)	S1'–C24'–C25'	118.7(3)
S1–C24–C29	123.6(3)	S1'–C24'–C29'	123.4(3)
Dihedral Angles (deg)			
S1–N1–C1–C6	–0.7(5)	S1'–N1'–C1'–C6'	–15.0(5)
S1–N1–C1–C2	177.9(2)	S1'–N1'–C1'–C2'	166.6(2)
C1–N1–S1–C24	–169.0(3)	C1'–N1'–S1'–C24'	–175.5(3)
N1–S1–C24–C25	171.4(3)	N1'–S1'–C24'–C25'	170.6(3)
N1–S1–C24–C29	–6.5(4)	N1'–S1'–C24'–C29'	–10.5(3)

The ORTEP drawing of **1b** is shown in Figure 4, and selected bond lengths, bond angles, and torsion angles are summarized in Table 3.

The X-ray crystallographic results show that there are two conformers in the crystals of **1b**. One is a syn form, and the other is an anti form. In the syn form the pyridyl nitrogen and ortho chlorine atom on the phenylthiyl benzene ring are on the same side with respect to the ring A–N–S–ring E π -framework of the radical molecule, and in the anti form they are on opposite sides from each other. The bond lengths and bond angles are nearly identical to each other, but the torsion angles are somewhat different. In the syn form the N1 and S1 atoms are coplanar with the A benzene ring within 0.027(3) Å, and this plane makes a dihedral angle of 15.9° to the E benzene ring. The dihedral angles between the A and B benzene rings, between the A and C benzene rings, and between the A benzene and D pyridine rings are 48.1, 77.0, and 35.7°, respectively, indicating that there is steric congestion around the radical center. On the other hand, the anti form adopts a somewhat less planar form. The torsion angles for S1'–N1'–C1'–C2' and S1'–N1'–C1'–C6' are –15.0(5) and 166.6(2)°, respectively, indicating that the anti form is more twisted about the C1'–N1' bond than the syn form [–0.7(5) and 177.9(2)°]. On the other hand, the torsion angles for C1'–N1'–S1'–C24' [–175.5(3)°], N1'–S1'–C25'–C26' [170.6(3)°], and N1'–S1'–C25'–C29' [–10.5(3)°] are nearly identical with those for the syn form [–169.0(3), 171.4(3), and –6.5(4)°]. The dihedral angles between the A' and B' benzene rings, between the A' and C' benzene rings, and between the A' benzene and D' pyridine rings are 50.0, 79.9, and 27.6°, respectively, which are similar to those for the syn form. In conclusion, the π -frameworks consisting of the benzene ring A (A'), N1 (N1'), S1 (S1'), and the benzene ring E (E') are approximately planar in both forms. Therefore, this planar form makes an extensive delocalization of the unpaired electron onto the anilino benzene ring and phenylthiyl group possible. In contrast, the large twistings (48.1–79.9°) of the B, B', C, and C' benzene rings from the planar π -framework will suppress delocalization of the unpaired electron onto those benzene rings. In fact, the ESR results of **18** and **19** indicate a very small or negligibly small delocalization of the unpaired electron onto the 2- and 6-benzene or pyridine rings. On the other hand, a small twisting angle of the 4-benzene or pyridine ring allows a small localization of the unpaired electron onto the 4-benzene or pyridine ring.

The magnetic properties of **1a**, **1b**, **2a**, and **2b** were investigated using polycrystalline samples in the temperature range 1.8–300 K on a SQUID magnetometer. The diamagnetic components were estimated using Pascal's constants. The radical purities of **1** and **2** were determined to be 98.5 (**1a**), 95.0 (**1b**), 93.0 (**2a**), and 99.0% (**2b**) from the magnetic susceptibility measurements.

Figure 5 shows the temperature dependence of $\chi_{\text{mol}}T$ for **2b**. The $\chi_{\text{mol}}T$ values are nearly constant in the temperature region above 50 K, and below this temperature, it increases drastically with decreasing temperature. This profile indicates that the intermolecular magnetic interaction is FM, and the $\chi_{\text{mol}}T$ vs T plots have been well analyzed using a one-dimensional (1D) regular Heisenberg model (eq 1)²⁶ with an interaction of $2J/k_B = 22.4$ K, as shown in Figure 5.

$$H = -2J \sum S_i \cdot S_j \quad (1)$$

(26) Bonner, J. C.; Fisher, M. E. *Phys. Rev.* **1964**, *A135*, 640.

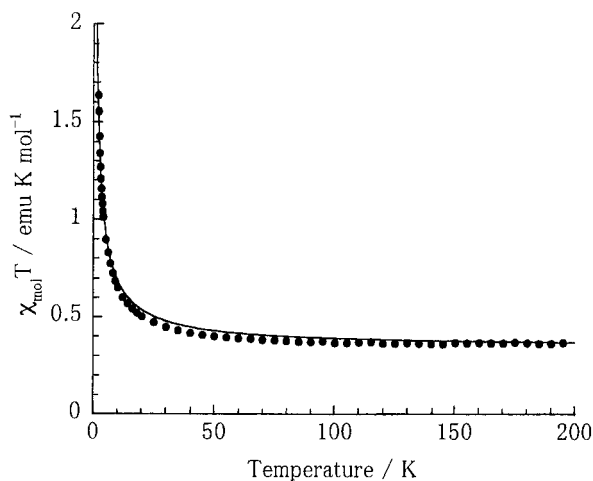


Figure 5. $\chi_{\text{mol}} T$ vs T plots for **2b**. The solid curve represents theoretical susceptibilities calculated with a 1D regular Heisenberg model with $2J/k_B = +22.4$ K.

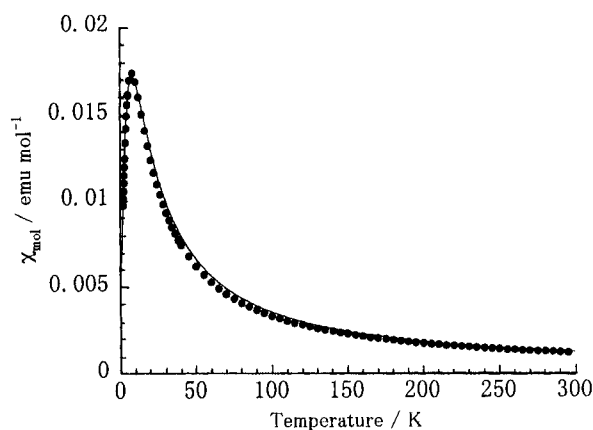


Figure 6. χ_{mol} vs T plots for **1b**. The solid curve represents theoretical susceptibilities calculated with a 1D alternating Heisenberg model with $2J/k_B = -12.8$ K and $\alpha = 0.91$.

The temperature dependence of χ_{mol} for **1b** is shown in Figure 6. As found in the figure, χ_{mol} increases gradually and reaches a maximum at 10 K with decreasing temperature. Then, it decreases with decreasing temperature. This profile indicates that the interaction between the neighboring spins is AFM. The χ_{mol} vs T plots were analyzed with an alternating linear-chain model (eq 2, where α is an alternation parameter),²⁷ and the best fit with the experiment gave $2J/k_B = -12.8$ K and $\alpha = 0.91$.

$$H = -2J \sum (S_{2i-1} \cdot S_{2i} + \alpha S_{2i} \cdot S_{2i+1}) \quad (2)$$

The crystal structure of **1b** is shown in Figure 7, which shows that the molecules are stacked alternately with the syn and anti forms along the crystallographic a axis. The SOMO–SOMO overlap between the neighboring molecules is along this direction which leads to antiferromagnetic exchange interaction between the unpaired electron spins.

The temperature dependence of χ_{mol} for **1a** is shown in Figure 8. χ_{mol} increases gradually and reaches a broad

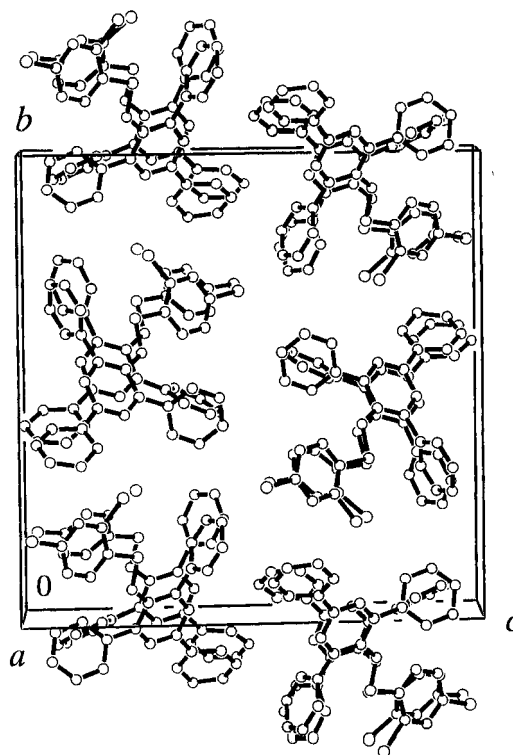


Figure 7. Crystal structure of **1b**.

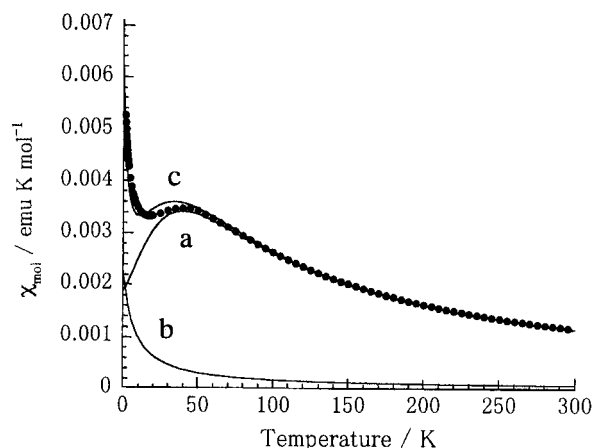


Figure 8. χ_{mol} vs T plots for **1a**. Solid curve a represents theoretical susceptibilities calculated with 1D AFM regular Heisenberg model with $2J/k_B = -63.4$ K, and curve b is calculated for 3.0% of a monoradical impurity following the Curie–Weiss law with $\theta = -2.0$ K. Curve c is a superposition of curves a and b.

maximum at 40 K with decreasing temperature. Then, χ_{mol} decreases gradually with decreasing temperature, and below 20 K it again increases. This increase of χ_{mol} below 20 K is probably due to the presence of isolated monoradicals which are randomly located in the lattice defects/or broken-chain edges. The contribution (x) of the monoradical impurity (curve b) is estimated to be ca. 3.0%, and the estimated Weiss constant (θ) is -2.0 K. The superposition of the theoretical curve of a 1D AFM regular Heisenberg model (curve a) and curve b based on eq 3, where C is the Curie constant, gives curve c.

$$H = -(1-x)2J \sum S_i \cdot S_j + xC/(T-\theta) \quad (3)$$

The best fit with the experiment gave $2J/k_B = -63.4$ K ($\alpha = 1$). A similar magnetic behavior was observed

(27) (a) Duffy, W. Jr.; Barry, K. P. *Phys. Rev.* **1968**, *165*, 647. (b) Hall, J. W.; March, W.; Weller, R. R.; Hatfield, W. E. *Inorg. Chem.* **1981**, *20*, 1033.

for **2a**. The best fit with the experiment using a 1D AFM regular Heisenberg model gave $2J/k_B = -17.8$ K. In this case paramagnetic impurity was nearly zero. Therefore, an increase in χ_{mol} in the low-temperature region was not observed.

Conclusion

Five kinds of pyridyl-substituted thioaminy radicals, **1a**, **1b**, **2a**, **2b**, and **3**, have been generated, and the former four radicals could be isolated as radical crystals. Radical **3** has been shown to be gradually decomposed in solution with a half-life time of 8 h at 20 °C. The X-ray crystallographic analysis of **1b** has shown that the Ar–N–S–Ar' π -framework is approximately planar, and the 2- and 6-phenyl groups are significantly twisted from this plane. The magnetic susceptibility measurements for the isolated radicals have showed that, although the intermolecular magnetic interactions of **1a** ($2J/k_B = -63.4$ K, $\alpha = 1.0$), **1b** (12.8 K, 0.91), and **2a** (-17.8 K, 1.0) are antiferromagnetic, that of **2b** is ferromagnetic and analysis of the susceptibility data with a 1D ferromagnetic regular Heisenberg model gave $2J/k_B = +22.4$ K.

Experimental Section

IR, UV–vis, and ¹H NMR measurements were performed as previously reported.¹⁷ ESR spectra were obtained with a Bruker ESP300 spectrometer equipped with an X-band microwave unit and 100 kHz field modulation. Hyperfine coupling constants (*a*) and *g* values were determined by simultaneous measurements with Fremy's salt ($a_N = 1.309$ mT, $g = 2.0057$) in an aqueous K₂CO₃ solution. Magnetic susceptibility (χ) measurements were carried out using polycrystalline samples in the temperature range 1.8–300 K with a Quantum Design MPMS2 SQUID magnetometer. The diamagnetic contributions were corrected using Pascal's constants. Column chromatography was carried out on silica gel (Fuji Silysia Chemical Ltd., BW-127ZH) or alumina (Merck, aluminum oxide 90).

Materials. 3-Bromopyridine and 4-aminopyridine are commercially available. Phenylboronic acid,²⁸ phenylboronic-*o*-₂ acid,¹⁹ diethyl(3-pyridyl)borane,²⁹ and Pd(PPh₃)₄³⁰ were obtained by the previously reported methods. 4-Aminobiphenyl was prepared by reduction of 4-nitrobiphenyl with Pd/C. 4-Nitrobenzenesulfonyl and 2,4-dichlorobenzenesulfonyl chlorides were prepared by bubbling Cl₂ gas into a suspension of 4,4'-dinitrodiphenyl disulfide or a solution of 2,4-dichlorothio-phenol in 20–30 mL of dichloromethane.³¹ After the resulting red solution was concentrated to ~3 mL under reduced pressure, they were used in the next step without further purification.¹⁷

4-(3-Pyridyl)aniline (7). A mixture of 3.44 g (20 mmol) of bromoaniline, 3.53 g (24 mmol) of diethyl(3-pyridyl)borane, 2.31 g (2.00 mmol) of Pd(PPh₃)₄, 3.22 g (10 mmol) of tetrabutylammonium bromide, and 5.28 g of KOH powder in 100 mL of anhydrous THF was refluxed with stirring for 24 h under nitrogen. It was then extracted with benzene, dried (MgSO₄), evaporated, and chromatographed on silica gel with ethyl acetate. Crystallization from hexane–benzene gave **7** in 68% yield as colorless prisms with mp 116–117 °C: IR (KBr) 3410 and 3260 cm⁻¹ (NH₂); ¹H NMR (CDCl₃) δ 3.64 (s, 2H), 6.78 (d, *J* = 8.3 Hz, 2H), 7.31 (dd, *J* = 4.9 and 7.9 Hz, 1H), 7.40 (d, *J* = 8.3 Hz, 2H), 7.81 (dt, *J* = 7.9 and 2.0 Hz, 1H), 8.50 (dd, *J* = 4.9 and 2.0 Hz, 1H), 8.80 (d, *J* = 2.0 Hz, 1H).

2,6-Dibromo-4-(3-pyridyl)aniline (8). A mixture of 1.66 g (9.8 mmol) of **7**, 11.5 g (29 mmol) of benzyltrimethylammonium tribromide (BTMA·Br₃), and 3.43 g of CaCO₃ in dichloromethane (200)–MeOH (80 mL) was stirred for 3 h at room temperature. After filtration, the filtrate was evaporated and dichloromethane was added. The dichloromethane layer was washed with 10% aqueous NaHSO₃, dried (MgSO₄), evaporated, and crystallized from hexane–benzene to give **8** in 88% yield as light red prisms with mp 114–115 °C: IR (KBr) 3430 and 3320 cm⁻¹ (NH₂); ¹H NMR (CDCl₃) δ 4.70 (s, 2H), 7.32 (dd, *J* = 7.8 and 4.9 Hz, 1H), 7.61 (s, 2H), 7.75 (dt, *J* = 7.8 and 2.0 Hz, 1H), 8.55 (dd, *J* = 4.9 and 2.0 Hz, 1H), 8.74 (d, *J* = 2.0 Hz, 1H).

2,6-Diphenyl-4-(3-pyridyl)aniline (9). A mixture of 2.95 g (9.0 mmol) of **8**, 2.85 g (23.0 mmol) of phenylboronic acid, 2.08 g (1.80 mmol) of Pd(PPh₃)₄, and 7.63 g of Na₂CO₃ in benzene (200)–EtOH (40)–H₂O (36 mL) was refluxed for 24 h with stirring under nitrogen. After 200 mL of benzene was added, the organic layer was washed with brine and dried (MgSO₄). Evaporation, column chromatography on silica gel with 5:1 benzene–ethyl acetate, and crystallization (MeOH) gave **9** in 57% yield (1.65 g, 5.13 mmol) as colorless plates with mp 130–132 °C: IR (KBr) 3450 and 3360 cm⁻¹ (NH₂); ¹H NMR (CDCl₃) δ 3.98 (s, 2H), 7.29 (dd, *J* = 7.8 and 4.9 Hz, 1H), 7.37 (t, *J* = 7.8 Hz, 2H), 7.38 (s, 2H), 7.48 (t, *J* = 7.8 Hz, 4H), 7.54 (d, *J* = 7.8 Hz, 4H), 7.85 (d, *J* = 7.8 Hz, 1H), 8.49 (d, *J* = 4.9 Hz, 1H), 8.85 (s, 1H). Anal. Calcd for C₂₃H₁₈N₂: C, 85.68; H, 5.63; N, 8.69. Found: C, 85.53; H, 5.68; N, 8.41.

N-[(4-Nitrophenyl)thio]-2,6-diphenyl-4-(3-pyridyl)aniline (4a). To a stirred solution of 0.97 g (3.00 mmol) of **9** and 2.0 mL of Et₃N in 80 mL of anhydrous THF at 0 °C was added dropwise a solution of 5.4 mmol of 4-nitrobenzenesulfonyl chloride in 10 mL of anhydrous THF. After the completion of addition, the mixture was stirred for 2 h at 0 °C, filtered, and evaporated, and the residue was column chromatographed on alumina with benzene. Crystallization from EtOH gave **4a** in 80% yield (1.14 g, 2.40 mmol) as yellow prisms with mp 158–160 °C: IR (KBr) 3320 cm⁻¹ (NH); ¹H NMR (CDCl₃) δ 5.45 (s, 1H), 6.88 (d, *J* = 8.8 Hz, 2H), 7.27–7.46 (m, 13H), 7.88 (d, *J* = 7.9 Hz, 1H), 7.89 (d, *J* = 8.8 Hz, 2H), 8.56 (d, *J* = 4.9 Hz, 1H), 8.85 (s, 1H). Anal. Calcd for C₂₉H₂₁N₃O₂S: C, 73.24; H, 4.45; N, 8.84. Found: C, 73.21; H, 4.67; N, 8.65.

N-[(2,4-Dichlorophenyl)thio]-2,6-diphenyl-4-(3-pyridyl)aniline (4b). To a stirred solution of 0.97 g (3.00 mmol) of **9** and 2.0 mL of Et₃N in 80 mL of anhydrous THF at 0 °C was added dropwise a solution of 5.4 mmol of 2,4-dichlorobenzenesulfonyl chloride in 10 mL of anhydrous THF. After the completion of addition, the mixture was stirred for 2 h at 0 °C, filtered, and evaporated, and the residue was column chromatographed on alumina with benzene. Crystallization from EtOH gave **4b** in 69% yield (1.03 g, 2.07 mmol) as colorless prisms with mp 129–130 °C: IR (KBr) 3320 cm⁻¹ (NH); ¹H NMR (CDCl₃) δ 5.33 (s, 1H), 6.90 (d, *J* = 8.8 Hz, 1H), 6.97 (dd, *J* = 8.8 and 2.0 Hz, 1H), 7.07 (d, *J* = 2.0 Hz, 1H), 7.28–7.42 (m, 13H), 7.87 (d, *J* = 7.8 Hz, 1H), 8.55 (d, *J* = 4.9 Hz, 1H), 8.85 (s, 1H). Anal. Calcd for C₂₉H₂₀Cl₂N₂S: C, 69.74; H, 4.04; N, 5.61. Found: C, 69.86; H, 4.16; N, 5.60.

2,6-Dibromo-4-phenylaniline (10). A mixture of 5.92 g (35 mmol) of 4-aminobiphenyl, 30.0 g (77 mmol) of BTMA·Br₃, and 8.76 g of CaCO₃ in dichloromethane (250)–MeOH (100 mL) was stirred for 2 h at room temperature. After the reaction mixture was evaporated, benzene was added, and the organic layer was washed with aqueous 10% NaHSO₃ and brine and dried (MgSO₄). Evaporation and crystallization (hexane–benzene) gave **10** in 97% yield as light brown prisms with mp 113–116 °C: IR (KBr) 3415 and 3305 cm⁻¹ (NH₂); ¹H NMR (CDCl₃) δ 4.57 (s, 2H), 7.29 (tt, *J* = 7.3 and 1.5 Hz, 1H), 7.38 (t, *J* = 7.3 Hz, 2H), 7.45 (dd, *J* = 7.3 and 1.5 Hz, 2H), 7.61 (s, 2H).

4-Phenyl-2,6-di(3-pyridyl)aniline (11). A mixture of 3.27 g (10.0 mmol) of **10**, 3.52 g (24 mmol) of diethyl(3-pyridyl)borane, 2.31 g (2.00 mmol) of Pd(PPh₃)₄, 5.28 g of KOH powder, and 3.22 g (10 mmol) of tetrabutylammonium bromide in 100 mL of THF was refluxed for 24 h with stirring under nitrogen. After benzene was added, the organic layer was washed with

(28) Washburn, R. M.; Levens, E.; Albright, C. F.; Billing, F. A. *Organic Syntheses*; Wiley: New York, 1963; Collect. Vol. IV, p 68.

(29) Terashima, M.; Kakimi, H.; Ishikura, M.; Kamata, K. *Chem. Pharm. Bull.* **1983**, *31*, 4573.

(30) Coulson, D. R. *Inorg. Synth.* **1972**, *13*, 121.

(31) Kühle, E. *Synthesis* **1970**, 561.

brine and dried (MgSO₄). Evaporation, column chromatography on silica gel with 9:1 ethyl acetate–EtOH, and crystallization (hexane–benzene) gave **11** in 42% yield (1.36 g, 4.20 mmol) as light brown prisms with mp 142–143 °C: IR (KBr) 3380 and 3300 cm⁻¹ (NH₂); ¹H NMR (CDCl₃) δ 3.83 (s, 2H), 7.41 (s, 2H), 7.30 (t, *J* = 7.3 Hz, 1H), 7.39–7.44 (m, 4H), 7.58 (d, *J* = 7.3 Hz, 2H), 7.90 (dt, *J* = 8.30 and 2.0 Hz, 2H), 8.65 (dd, *J* = 4.9 and 2.0 Hz, 2H), 8.81 (d, *J* = 2.0 Hz, 2H). Anal. Calcd for C₂₂H₁₇N₃: C, 81.71; H, 5.30; N, 12.99. Found: C, 81.90; H, 5.70; N, 12.90.

N-[(4-Nitrophenyl)thio]-4-phenyl-2,6-di(3-pyridyl)aniline (5a). To a stirred solution of 0.97 g (3.00 mmol) of **11** and 2.0 mL of Et₃N in 80 mL of anhydrous THF at 0 °C was added dropwise a solution of 6.0 mmol of 4-nitrobenzenesulfenyl chloride in 20 mL of anhydrous THF. After the completion of addition, the mixture was stirred for 2 h at 0 °C, filtered, evaporated, and column chromatographed on alumina with 1:2 ethyl acetate–benzene. Crystallization from hexane–benzene gave **5a** in 68% yield (0.972 g, 2.04 mmol) as yellow prisms with mp 186–188 °C: IR (KBr) 3220 cm⁻¹ (NH); ¹H NMR (CDCl₃) δ 5.19 (s, 1H), 6.93 (d, *J* = 8.8 Hz, 2H), 7.24 (dd, *J* = 8.5 and 4.9 Hz, 2H), 7.35 (t, *J* = 7.3 Hz, 1H), 7.43 (t, *J* = 7.3 Hz, 2H), 7.47 (s, 2H), 7.59 (d, *J* = 7.3 Hz, 2H), 7.76 (dt, *J* = 8.5 and 2.0 Hz, 2H), 7.95 (d, *J* = 8.8 Hz, 2H), 8.50 (dd, *J* = 4.9 and 2.0 Hz, 2H), 8.72 (d, *J* = 2.0 Hz, 2H). Anal. Calcd for C₂₈H₂₀N₄O₂S: C, 70.57; H, 4.23; N, 11.76. Found: C, 70.76; H, 4.45; N, 11.49.

N-[(2,4-Dichlorophenyl)thio]-4-phenyl-2,6-di(3-pyridyl)aniline (5b). To a stirred solution of 0.97 g (3.00 mmol) of **11** and 2.0 mL of Et₃N in 80 mL of anhydrous THF at 0 °C was added dropwise a solution of 6.0 mmol of 2,4-dichlorobenzenesulfenyl chloride in 10 mL of anhydrous THF. After the completion of addition, the mixture was stirred for 2 h at 0 °C, filtered, evaporated, and column chromatographed on alumina with 1:1 ethyl acetate–benzene. Recrystallization from hexane–benzene gave **5b** in 74% yield (1.11 g, 2.22 mmol) as colorless prisms with mp 179–180 °C: IR (KBr) 3200 cm⁻¹ (NH); ¹H NMR (CDCl₃) δ 5.12 (s, 1H), 6.91 (d, *J* = 8.3 Hz, 1H), 7.03 (dd, *J* = 8.3 and 2.0 Hz, 1H), 7.12 (d, *J* = 2.0 Hz, 1H), 7.26 (dd, *J* = 7.8 and 4.6 Hz, 2H), 7.34 (t, *J* = 7.3 Hz, 1H), 7.43 (t, *J* = 7.3 Hz, 2H), 7.45 (s, 2H), 7.58 (d, *J* = 7.3 Hz, 2H), 7.73 (dt, *J* = 7.8 and 2.0 Hz, 2H), 8.53 (dd, *J* = 4.6 and 2.0 Hz, 2H), 8.67 (d, *J* = 2.0 Hz, 2H). Anal. Calcd for C₂₈H₁₉Cl₂N₃S: C, 67.20; H, 3.83; N, 8.40. Found: C, 67.44; H, 4.03; N, 8.18.

4-Amino-3,5-dibromopyridine (12). To a stirred solution of 9.4 g (100 mmol) of 4-aminopyridine in 40 mL of acetic acid at 80 °C was added a solution of 34 g (210 mmol) of Br₂ in 20 mL of acetic acid over 1 h. After being stirred for 14 h at the same temperature, the reaction mixture was washed with aqueous Na₂S₂O₃ and neutralized with 10% NaOH. The mixture was then extracted with CH₂Cl₂, and the extract was washed with brine and dried (MgSO₄). Evaporation, chromatography on alumina with 1:1 benzene–ethyl acetate, and crystallization (hexane–benzene) gave **12** as colorless needles in 14% yield (3.53 g, 14.0 mmol): IR (KBr) 3430 and 3265 cm⁻¹ (NH₂); ¹H NMR (CDCl₃) δ 5.08 (s, 2H), 8.31 (s, 2H).

4-Amino-3,5-diphenylpyridine (13). A mixture of 3.02 g (12.0 mmol) of **12**, 3.80 g (31.0 mmol) of phenylboronic acid, 1.66 g (1.44 mmol) of Pd(PPh₃)₄, and 10.2 g of Na₂CO₃ in benzene (150)–EtOH (30)–H₂O (50 mL) was refluxed for 24 h with stirring under nitrogen. After benzene was added, the organic layer was washed with brine and dried (MgSO₄). Evaporation, column chromatography on silica gel with ethyl acetate, and crystallization (hexane–benzene) gave **13** in 52% yield (1.54 g, 6.24 mmol) as colorless prisms with mp 150–151 °C: IR (KBr) 3480 and 3310 cm⁻¹ (NH₂); ¹H NMR (CDCl₃) δ 4.48 (s, 2H), 7.43–7.53 (m, 10H), 8.17 (s, 2H). Anal. Calcd for C₁₇H₁₄N₂: C, 82.90; H, 5.73; N, 11.37. Found: C, 83.09; H, 5.79; N, 11.09.

N-[(2,4-Dichlorophenyl)thio]-2,6-diphenyl(4-pyridyl)amine (6). To a stirred solution of 0.99 g (4.00 mmol) of **13** and 2.0 mL of Et₃N in 50 mL of anhydrous THF was added dropwise a solution of 6.0 mmol of 2,4-dichlorobenzenesulfenyl chloride in 10 mL of anhydrous THF. After the completion of

addition, the mixture was stirred for 2 h at 0 °C, filtered, evaporated, and column chromatographed on alumina with benzene. Recrystallization from hexane–benzene gave **6** in 52% yield (0.88 g, 2.08 mmol) as colorless prisms with mp 120–122 °C: IR (KBr) 3150 cm⁻¹ (NH); ¹H NMR (CDCl₃) δ 5.62 (s, 1H), 6.84 (d, *J* = 8.3 Hz, 1H), 7.05 (dd, *J* = 8.3 and 2.0 Hz, 1H), 7.10 (d, *J* = 2.0 Hz, 1H), 7.33–7.39 (m, 10H), 8.27 (s, 2H). Anal. Calcd for C₂₃H₁₆Cl₂N₂S: C, 65.25; H, 3.81; N, 6.62. Found: C, 65.63; H, 4.20; N, 6.25.

Isolation of Radicals. To a stirred solution of 200 mg of **4** or **5** in 20 mL (**4a** and **4b**) or 40 mL (**5a** and **5b**) of benzene was added 2.0 g of K₂CO₃. PbO₂ (7.00 g for **3a** and **3b**, and 8.0 g for **5a** and **5b**) was then added in 6–8 portions during 2 min, and stirring was continued for additional 1 min. After filtration, the solvent was removed by freeze-drying, and the greenish crystalline residue was crystallized from hexanes–ethyl acetate (**1a**, **1b**, **2b**) or EtOH (**2a**).

N-[(4-Nitrophenyl)thio]-2,6-diphenyl-4-(3-pyridyl)phenylaminyl (1a): dark green fine prisms; yield 19%; mp 170–171 °C. Anal. Calcd for C₂₉H₂₀N₃O₂S: C, 73.40; H, 4.25; N, 8.85. Found: C, 73.27; H, 4.14; N, 8.81.

N-[(2,4-Dichlorophenyl)thio]-2,6-diphenyl-4-(3-pyridyl)phenylaminyl (1b): dark green needles; yield 25%; mp 135–137 °C. Anal. Calcd for C₂₉H₁₉Cl₂N₂S: C, 69.88; H, 3.84; N, 5.62. Found: C, 69.59; H, 3.92; N, 5.55.

N-[(4-Nitrophenyl)thio]-4-phenyl-2,6-di(3-pyridyl)phenylaminyl (2a): dark green fine plates; yield 38%; mp 156–158 °C. Anal. Calcd for C₂₈H₁₉N₄O₂S: C, 70.72; H, 4.03; N, 11.78. Found: C, 70.54; H, 4.07; N, 11.60.

N-[(2,4-Dichlorophenyl)thio]-4-phenyl-2,6-di(3-pyridyl)phenylaminyl (2b): dark green fine needles; yield 31%; mp 125–127 °C. Anal. Calcd for C₂₈H₁₈Cl₂N₃S: C, 67.34; H, 3.63; N, 8.41. Found: C, 67.42; H, 3.78; N, 8.22.

2,6-Di(phenyl-d₅)-4-(3-pyridyl)aniline. A mixture of 1.97 g (6.00 mmol) of **8**, 1.83 g (14.4 mmol) of phenylboronic-d₅ acid, 1.39 g (1.20 mmol) of Pd(PPh₃)₄, and 5.09 g of Na₂CO₃ in benzene (83)–EtOH (15)–H₂O (24 mL) was refluxed for 24 h with stirring under nitrogen. The usual workup and subsequent column chromatography (1:5 ethyl acetate–benzene) and crystallization (MeOH) gave 2,6-di(phenyl-d₅)-4-(3-pyridyl)aniline as colorless plates with mp 126–128 °C in 45% yield (0.90 g, 2.7 mmol): IR (KBr) 3440 and 3300 (NH₂), 2280 cm⁻¹ (C–D); ¹H NMR (CDCl₃) δ 4.00 (s, 2H), 7.31 (dd, *J* = 7.8 and 4.9 Hz, 1H), 7.39 (s, 2H), 7.88 (dt, *J* = 7.8 and 2.0 Hz, 1H), 8.51 (dd, *J* = 4.9 and 2.0 Hz, 1H), 8.86 (d, *J* = 2.0 Hz, 1H). Anal. Calcd for C₂₃H₈D₁₀N₂: C, 83.10; H + D, 5.46; N, 8.43. Found: C, 82.78; H + D, 5.59; N, 8.00.

N-[(2,4-Dichlorophenyl)thio]-2,6-di(phenyl-d₅)-4-(3-pyridyl)aniline (16). To a stirred solution of 0.66 g (1.99 mmol) of 2,6-di(phenyl-d₅)-4-(3-pyridyl)aniline and 1.0 mL of Et₃N in 65 mL of anhydrous THF at 0 °C was added dropwise a solution of 2.99 mmol of 2,4-dichlorobenzenesulfenyl chloride in 10 mL of anhydrous THF. After being stirred at 0 °C for 2 h, the reaction mixture was filtered, evaporated, and column chromatographed on alumina with benzene. Crystallization from EtOH gave **16** as colorless prisms with mp 139–141 °C in 65% yield (0.66 g, 1.29 mmol): IR (KBr) 3340 (NH), 2270 cm⁻¹ (C–D); ¹H NMR (CDCl₃) δ 5.33 (s, 1H), 6.90 (d, *J* = 8.8 Hz, 1H), 6.97 (dd, *J* = 8.8 and 2.0 Hz, 1H), 7.07 (d, *J* = 2.0 Hz, 1H), 7.33 (dd, *J* = 7.8 and 4.9 Hz, 1H), 7.42 (s, 2H), 7.87 (dt, *J* = 7.8 and 2.0 Hz, 1H), 8.55 (dd, *J* = 4.9 and 2.0 Hz, 1H), 8.85 (d, *J* = 2.0 Hz, 1H). Anal. Calcd for C₂₃H₁₀Cl₂D₁₀N₂S: C, 68.37; H + D, 3.96; N, 5.50. Found: C, 68.24; H + D, 4.22; N, 5.27.

4-(Phenyl-d₅)aniline. A mixture of 5.16 g (30.0 mmol) of 4-bromoaniline, 4.95 (39.0 mmol) of phenylboronic-d₅ acid, 3.47 g (3.00 mmol) of Pd(PPh₃)₄, and 12.7 g of Na₂CO₃ in benzene (170)–EtOH (30)–H₂O (60 mL) was gently refluxed for 24 h with stirring under nitrogen. The usual workup and subsequent crystallization (EtOH) gave 4-(phenyl-d₅)aniline in 82% yield (4.28 g, 24.6 mmol) as colorless plates with mp 54–56 °C: IR (KBr) 3430, 3400, 3330, and 3200 (NH₂), 2280 and 2270 cm⁻¹ (C–D); ¹H NMR (CDCl₃) δ 6.75 (d, *J* = 8.3 Hz, 2H), 7.41 (d, *J* = 8.3 Hz, 2H).

2,6-Dibromo-4-(phenyl-*d*₅)aniline. A mixture of 3.91 g (22.4 mmol) of 4-(phenyl-*d*₅)aniline, 21.0 g (54 mmol) of BTMA·Br₃, and 6.7 g of CaCO₃ in CH₂Cl₂ (150)–MeOH (60 mL) was stirred at room temperature for 2 h. The usual workup and subsequent crystallization (hexane–benzene) gave 2,6-dibromo-4-(phenyl-*d*₅)aniline as light brown prisms with mp 116–118 °C in 93% yield (6.92 g, 20.8 mmol): IR (KBr) 3410 and 3300 (NH₂), 2280 and 2270 cm⁻¹ (C–D); ¹H NMR (CDCl₃) δ 4.59 (br s, 2H), 7.63 (s, 2 H).

4-(Phenyl-*d*₅)-2,6-di(3-pyridyl)aniline. A mixture of 5.07 g (15.3 mmol) of 2,6-dibromo-4-(phenyl-*d*₅)aniline, 5.84 g (39.7 mmol) of diethyl(3-pyridyl)borane, 3.54 g (3.06 mmol) of Pd(PPh₃)₄, 8.06 g of KOH powder, and 4.92 g (15.3 mmol) of tetrabutylammonium bromide in 155 mL of THF was gently refluxed for 24 h with stirring under nitrogen. After the usual workup, the reaction mixture was chromatographed with 1:9 EtOH–ethyl acetate, and crystallization from hexane–benzene gave 2,6-di(phenyl-*d*₅)-4-(3-pyridyl)aniline as colorless prisms with mp 143–144 °C in 41% yield (2.06 g, 6.3 mmol): IR (KBr) 3370 and 3320 (NH₂), 2280 cm⁻¹ (C–D); ¹H NMR (CDCl₃) δ 3.82 (s, 2 H), 7.36 (s, 2 H), 7.44 (dd, *J* = 7.8 and 4.9 Hz, 2 H), 7.91 (dt, *J* = 7.8 and 2.0 Hz, 2 H), 8.66 (dd, *J* = 4.9 and 2.0 Hz, 2 H), 8.82 (d, *J* = 2.0 Hz, 2 H). Anal. Calcd for C₂₂H₁₂D₅N₃: C, 80.46; H + D, 5.22; N, 12.79. Found: C, 80.13; H + D, 5.77; N, 13.00.

***N*[(2,4-Dichlorophenyl)thio]-4-(phenyl-*d*₅)-2,6-di(3-pyridyl)aniline (17).** To a stirred solution of 1.31 g (4.00 mmol) of 4-(phenyl-*d*₅)-2,6-di(3-pyridyl)aniline and 2.0 mL of Et₃N in 120 mL of anhydrous THF at 0 °C was added dropwise a solution of 6.0 mmol of 2,4-dichlorobenzenesulfonyl chloride in 10 mL of anhydrous THF. After being stirred at 0 °C for 2 h, the reaction mixture was filtered, evaporated, and column chromatographed on alumina with 1:1 benzene–ethyl acetate. Crystallization from hexane–benzene gave **17** as colorless prisms with mp 177–179 °C in 70% yield (1.42 g, 2.81 mmol): IR (KBr) 3200 (NH), 2280 cm⁻¹ (C–D); ¹H NMR (CDCl₃) δ 5.09 (s, 1 H), 6.91 (d, *J* = 8.3 Hz, 1 H), 7.03 (dd, *J* = 8.3 and 2.0 Hz, 1 H), 7.12 (d, *J* = 2.0 Hz, 1 H), 7.26 (dd, *J* = 7.8 and 4.9 Hz, 2 H), 7.45 (s, 2 H), 7.73 (dt, *J* = 7.8 and 2.0 Hz, 2 H), 8.54 (dd, *J* = 4.9 and 2.0 Hz, 2 H), 8.67 (d, *J* = 2.0 Hz, 2 H). Anal. Calcd for C₂₈H₁₄Cl₂D₅N₃S: C, 66.53; H + D, 3.79; N, 8.31. Found: C, 66.88; H + D, 4.14; N, 7.94.

X-ray Crystallographic Analysis for **1b.**^{32,33} A dark green prismatic crystal of C₂₉H₁₉Cl₂N₂S (*M* = 498.45) having approximate dimensions of 0.70 × 0.15 × 0.15 mm was mounted on a glass fiber. All measurements were made on a Rigaku AFC7R diffractometer with graphite-monochromated Cu Kα radiation (*λ* = 1.541 78 Å): monoclinic space group *P*2₁/*c*, *a* = 10.591(2), *b* = 21.747(1), and *c* = 21.665(1) Å, β = 99.775(7)°, *V* = 4917.3(8) Å³, *Z* = 8, and *D*_c = 1.346 g cm⁻³.

The data were collected at a temperature of 23 ± 1 °C using the ω–2θ scan technique to a maximum 2θ value of 113.2°. The linear absorption coefficient, μ, for Cu Kα radiation is 33.2 cm⁻¹. An empirical absorption correction based on azimuthal scans of several reflections was applied which resulted in transmission factors ranging from 0.79 to 1.00.

The structure was solved by heavy-atom Patterson methods and expanded using Fourier techniques. The non-hydrogen atoms were refined anisotropically. All hydrogen atoms except one were refined isotropically, and the one was placed in the fixed position. Of the 6770 reflections collected, 4662 reflections with *I* > 3.00σ(*I*) were observed. The final cycle of full-matrix least-squares refinement was based on the observed reflections and 761 variable parameters and converged with unweighted and weighted agreement factors of *R* = 0.040 and *R*_w = 0.030.

Acknowledgment. The authors are grateful to Professor K. Matsumoto, Osaka City University, for valuable suggestions during X-ray crystallographic measurements.

Supporting Information Available: X-ray crystallographic data and ORTEP drawings and crystal structures for **1b** (18 pages). This material is contained in libraries on microfiche, immediately follows this article in the microfilm version of the journal, and can be ordered from the ACS; see any current masthead page for ordering information.

JO981155G

(32) The crystallographic computing was done by the TEXSAN structure analysis software.

(33) The authors have deposited atomic coordinations for this structure with the Cambridge Crystallographic Data Center. The coordinations can be obtained, on request, from the Director, Cambridge Crystallographic Data Center, 12 Union Road, Cambridge, CB2 1EZ, U.K.